

# UCSF

## UC San Francisco Previously Published Works

### Title

Characterization of the Acyl-Adenylate Linked Metabolite of Mefenamic Acid

### Permalink

<https://escholarship.org/uc/item/2qk7b4kz>

### Journal

Chemical Research in Toxicology, 26(3)

### ISSN

0893-228X

### Authors

Hornig, Howard

Benet, Leslie Z

### Publication Date

2013-03-18

### DOI

10.1021/tx300520j

Peer reviewed



Published in final edited form as:

*Chem Res Toxicol.* 2013 March 18; 26(3): 465–476. doi:10.1021/tx300520j.

## Characterization of the Acyl-Adenylate Linked Metabolite of Mefenamic Acid

Howard Horng and Leslie Z. Benet

Department of Bioengineering and Therapeutic Sciences, University of California, San Francisco

### Abstract

Mefenamic acid, (MFA), a carboxylic acid-containing nonsteroidal anti-inflammatory drug (NSAID), is metabolized into the chemically-reactive conjugates MFA-1-*O*-acyl-glucuronide (MFA-1-*O*-G) and MFA-*S*-acyl-CoA (MFA-CoA), which are both implicated in the formation of MFA-*S*-acyl-glutathione (MFA-GSH) conjugates, protein-adduct formation and thus the potential toxicity of the drug. However, current studies suggest that an additional acyl-linked metabolite may be implicated in the formation of MFA-GSH. In the present study, we investigated the ability of MFA to become bioactivated into the acyl-linked metabolite, mefenamyl-adenylate (MFA-AMP). In vitro incubations in rat hepatocytes with MFA (100  $\mu$ M), followed by LC-MS/MS analyses of extracts, led to the detection of MFA-AMP. In these incubations, the initial rate of MFA-AMP formation was rapid, leveling off at a maximum concentration of 90.1 nM (20 sec), while MFA-GSH formation increased linearly, reaching a concentration of 1.7  $\mu$ M after 60 min incubation. In comparison, MFA-CoA was undetectable in incubation extracts until the 4 min time point, achieving a concentration of 45.6 nM at the 60 min time point, MFA-1-*O*-G formation was linear attaining a concentration of 42.2  $\mu$ M after 60 min incubation. In vitro incubation in buffer with the model nucleophile glutathione (GSH) under physiological conditions showed MFA-AMP to be reactive towards GSH, but 11-fold less reactive than MFA-CoA, while MFA-1-*O*-G exhibited little reactivity. However, in the presence of glutathione-*S*-transferase (GST), MFA-AMP mediated formation of MFA-GSH increased 6-fold, while MFA-CoA mediated formation of MFA-GSH only increased 1.4-fold. Collectively, in addition to the MFA-1-*O*-G, these results demonstrate that mefenamic acid does become bioactivated by acyl-CoA synthetase enzyme(s) in vitro in rat hepatocytes into the reactive transacylating derivatives MFA-AMP and MFA-CoA, both of which contribute to the transacylation of GSH and may be involved in the formation of protein adducts and potentially elicit an idiosyncratic toxicity.

### Keywords

mefenamic acid; acyl adenylates; *S*-acyl-CoA; acyl glucuronides; *S*-acyl-glutathione; bioactivation

### Introduction

Xenobiotic carboxylic acid drugs are a commonly encountered class of therapeutic agents that are widely used for a number of different treatments. Although generally well tolerated, carboxylic acid-containing drugs are associated with severe, sometimes fatal idiosyncratic toxicities.<sup>1, 2</sup> These toxicities are hypothesized to occur when carboxylic acid containing

---

Correspondence: Leslie Z. Benet, Ph.D., University of California, San Francisco, Department of Bioengineering and Therapeutic Sciences, 533 Parnassus Ave., Room U-68, San Francisco, CA 94143-0912, Leslie.Benet@ucsf.edu.

The authors declare no competing financial interests.

drugs undergo bioactivation into chemically reactive metabolites capable of transacylating protein nucleophiles. This covalent modification of tissue proteins by reactive intermediates is a possible mechanism for the idiosyncratic toxicity commonly associated with liver damage, skin reaction, renal toxicity, fever, rash, and eosinophilia.<sup>3,4</sup> Although, the overall incidence of acidic drug induced toxicity is low<sup>5-7</sup>, this phenomenon has become a major concern clinically.

The nonsteroidal anti-inflammatory drug (NSAID), mefenamic acid (MFA), 2-(2, 3-dimethylphenylamino) benzoic acid, has been implicated with a rare, but sometimes serious idiosyncratic hepato- and nephrotoxicity.<sup>8</sup> A proposed mechanism for the development of these toxicities suggests that MFA is metabolized to chemically-reactive metabolites that become covalently bound to tissue proteins leading to adverse immunological responses (Figure 1). In addition to the cytochrome P450 mediated formation of the 3-hydroxy-MFA<sup>9</sup> and the 3-carboxy-MFA<sup>10</sup>, MFA is metabolized into the MFA-1-*O*-acyl-glucuronide (MFA-1-*O*-G), an unstable and reactive acyl glucuronide metabolite<sup>8</sup> capable of covalently binding onto human serum albumin<sup>11</sup> and thus may be implicated in MFA mediated idiosyncratic toxicity. Acyl glucuronides of acidic drugs are proposed to bind covalently to protein via two different mechanisms. The first involves a direct transacylation reaction in which protein nucleophiles react with the carbonyl-carbon of the acyl glucuronide, resulting in a drug-protein conjugate. The second mechanism requires prior acyl migration of the drug moiety to permit the opening of the sugar ring, causing the resulting exposed reactive aldehyde group to reversibly form an imine (Schiff's base) with an amine group on proteins. Subsequent Amadori rearrangement then yields a stable ketoamine derivative in which both the drug and the glucuronic acid moiety become covalently bound onto the protein.<sup>12</sup> It is proposed that these drug-protein adducts act as immunogens and are recognized by the immune system as foreign, eliciting an autoimmune type response resulting in the associated idiosyncratic toxicity. Reactive species derived from carboxylic acid containing drugs can also react with GSH, which is considered a detoxification process by preventing covalent binding to intracellular macromolecules.<sup>13-19</sup> In addition to the reactive acyl glucuronide, MFA also forms thioester-linked acyl-coenzyme A (acyl-CoA) derivatives via the acyl-CoA synthetase, which are proposed to possess an increased chemical electrophilicity of their carbonyl-carbon upon their formation resulting in the transacylation of biological nucleophiles.<sup>20</sup> Prior to the formation of the acyl-CoAs, acyl-adenylate (AMP)-linked intermediates are formed when the adenosine monophosphate (AMP) moiety of ATP is covalently transferred to the carboxyl group of the substrate. The AMP moiety is then subsequently displaced with CoA to form acyl-CoA thioesters.<sup>21, 22</sup> Acyl-AMP are also believed to possess an increased carbonyl-carbon electrophilicity resulting in their reaction with protein nucleophiles.<sup>23, 24</sup> Acyl-AMP derivatives of cholic acid have been shown to be quantitatively important reactive intermediates.<sup>23, 25</sup>

In the present studies we characterized MFA-AMP and investigated its contribution to the metabolic activation pathways of MFA and its ability to transacylate glutathione (GSH) *in vitro* in rat hepatocytes in comparison to MFA-1-*O*-G and MFA-CoA. We propose that in addition to MFA-1-*O*-G, MFA undergoes bioactivation into MFA-CoA via the MFA-AMP intermediate, all of which contribute to the transacylation of GSH *in vitro* forming MFA-GSH and conceivably the formation of drug-protein adducts. If this proposal is correct, these reactive intermediates would indeed be predicted to be important in the formation of potentially immunogenic protein adducts *in vivo*, possibly leading to the idiosyncratic toxicity of MFA and other carboxylic acid-containing drugs.

## Materials and Methods

### Materials

MFA, adenosine monophosphate (AMP), coenzyme A (CoA), anhydrous tetrahydrofuran (THF), triethylamine (TEA), ethyl chloroformate (ECF), *N,N'*-dicyclohexylcarbodiimide, pyridine, potassium phosphate, potassium carbonate, dimethyl sulfoxide (DMSO), carbamazepine (CBZ), L-glutathione (GSH), and equine liver glutathione-*S*-transferase (GST) were all purchased from Sigma-Aldrich Chemical Co (St. Louis, MO). Acetonitrile (ACN), methanol, acetone, ammonium acetate, and ethyl acetate were all purchased from Fisher Scientific (Pittsburgh, PA). MFA-1-*O*-G was purchased from Toronto Research Chemicals (TRC) Inc. (North York, Ontario). All solvents used for HPLC and LC-MS/MS analysis were of chromatographic grade. Williams Media E and L-glutamine were purchased from Gibco (Grand Island, NY). Sprague-Dawley rats were purchased from Charles River (Wilmington, MA). Stock solutions of MFA-AMP, MFA-CoA, MFA-GSH and MFA-1-*O*-G were all prepared as 1 mM solutions in DMSO.

### Instrumentation and Analytical Methods

HPLC/UV was carried out on a Hewlett Packard 1100 series binary pump HPLC system (Santa Clara, CA) coupled to a Hewlett Packard 1100 UV-Vis detector. HP Chemstation software was used for the acquisition of all HPLC/UV data. LC-MS/MS analyses of synthetic standards and in vitro samples was performed on a Shimadzu LC-20AD (Kyoto, Japan) HPLC system coupled to an Applied Biosystem/MDS Sciex API (Framingham, MA) 4000 triple quadrupole mass spectrometer outfitted with a Turbo V ion source using positive ionization mode. All analytical LC-MS/MS analyses were performed on a reverse phase column (XTerra C-18, 5.0  $\mu$ m, 4.6  $\times$  150 mm, Milford, MA). The detection of MFA, MFA-AMP, MFA-CoA, MFA-1-*O*-G, and MFA-GSH was obtained using electrospray (ESI) positive ionization and a gradient system of aqueous ammonium acetate (10 mM, pH 5.6) and acetonitrile, 5% ACN (v/v) to 100% (v/v) over 15 min at a flow rate of 0.5 ml/min. Electrospray positive ionization was employed with a needle potential held at 5.5 kV. MS/MS tandem conditions utilized 2 mTorr argon collision gas and a collision potential of 89 eV. The acquisition of mass spectral data was acquired with Analyst software (version 1.5.2, AB Sciex, Framingham, MA). NMR spectra were acquired in DMSO-*d*<sub>6</sub> on a 300-MHz Bruker Avance spectrometer (Woodlands, TX) and analyzed using Topspin software.

### Synthesis of MFA-AMP Derivative

The synthesis of MFA-AMP was carried out with a solution consisting of 110 mg *N,N'*-dicyclohexylcarbodiimide in 0.4 ml pyridine.<sup>23</sup> The *N,N'*-dicyclohexylcarbodiimide solution was added to a solution consisting of MFA (0.49 mmol), and AMP (0.49 mmol) in 75% (v/v) pyridine. The reaction mixture was stirred at 4°C for 7 hr. The reaction mixture was then centrifuged at 3000 rpm for 5 min to remove any *N*-acylurea derivatives. The supernatant was then transferred to another culture tube followed by the addition of acetone (10 ml). The resulting precipitate was isolated by centrifugation at 3000 rpm for 5 min followed by further washes with acetone (10  $\times$  10 ml) and acidified water (pH 4–5) (10  $\times$  10 ml). The precipitate was dissolved in 0.1 M potassium phosphate buffer (pH 6) and underwent continued liquid-liquid washes with ethyl acetate (10  $\times$  10 ml). After removal of the ethyl acetate, one drop of 1N HCl was added to the aqueous solution to precipitate MFA-AMP, followed by further washes with acetone (10  $\times$  10 ml). The MFA-AMP precipitate was blown down to dryness using N<sub>2</sub> gas and then weighed out for preparation of a 1 mM MFA-AMP solution in DMSO. The MFA-AMP eluted at a retention time of 7.6 min (Figure 2A) and showed no impurities when analyzed by HPLC/UV (wavelengths: 220, 254, 262, and 280 nm), LC-MS analyses via reverse-phase gradient elution (as described above), <sup>1</sup>H, and <sup>13</sup>C NMR. Tandem LC-MS/MS analysis of MFA-AMP revealed (CID of MH<sup>+</sup> ion at m/

z 571), m/z (%) yielded: m/z 224 ( $[M + H - AMP]^+$ , 100%), m/z 136( $[\text{adenine} + H]^+$ , 28%), m/z 207 ( $[M + H - 364]^+$ , 25%) (Figure 3A).  $^1\text{H}$  NMR analysis of MFA-AMP (300MHz, DMSO- $d_6$ ):  $\delta$  2.09 (3H, s, mefenamyl,  $-CH_3$ ), 2.28 (3H, s, mefenamyl,  $-CH_3$ ), 4.08 (3H, m, ribofuranose,  $-OCH-$ ,  $-CH_2-$ ), 4.23 (1H, dd, ribofuranose,  $-CHOH$ ), 4.63 (1H, dd, ribofuranose,  $-CHOH$ ), 5.94 (1H, d, ribofuranose,  $-OCHN-$ ), 6.62 (2H, m, mefenamyl,  $ArH$ ), 7.03 (1H, dd, mefenamyl,  $ArH$ ), 7.10 (2H, m, mefenamyl,  $ArH$ ), 7.28 (3H, m, mefenamyl,  $ArH$  and adenosine  $NH_2$ ), 7.83 (1H, d, mefenamyl,  $ArH$ ), 8.13 (1H, s, adenosine,  $-CH$ ), 8.50 (1H, s, adenosine,  $-CH$ ), 9.35 (1H, s, mefenamyl,  $-NH$ ).  $^{13}\text{C}$  NMR of MFA-AMP (DMSO- $d_6$ ):  $\delta$  14.2 (mefenamyl,  $-CH_3$ ), 20.7 (mefenamyl,  $-CH_3$ ), 65.9 (ribofuranose,  $-CH_2-$ ), 71.4 (ribofuranose,  $-CHOH-$ ), 74.4 (ribofuranose,  $-CHOH-$ ), 84.5 (ribofuranose,  $-CHO-$ ), 87.3 (ribofuranose,  $-CHN-$ ), 112.1 (mefenamyl,  $-CCOO-$ ), 113.5 (mefenamyl,  $Ar-CH-$ ), 116.6 (mefenamyl,  $Ar-CH-$ ), 119.3 (adenosine,  $-NCC-$ ), 123.0 (mefenamyl,  $Ar-CH-$ ), 126.5 (mefenamyl,  $Ar-CH-$ ), 127.0 (mefenamyl,  $Ar-CH-$ ), 132.0 (mefenamyl,  $Ar-CH-$ ), 132.5 (mefenamyl,  $Ar-CMe-$ ), 134.8 (mefenamyl,  $Ar-CH-$ ), 138.4 (mefenamyl,  $Ar-CNH-$ ), 138.7 (mefenamyl,  $Ar-CMe-$ ), 139.9 (adenosine,  $-NCHN-$ ), 149.5 (mefenamyl,  $Ar-CNH-$ ), 150.1 (adenosine,  $-NCN-$ ), 152.9 (adenosine,  $-NCHN-$ ), 156.3 (adenosine,  $-CNH_2$ ), 165.9 (mefenamyl,  $-COO-$ ). NMR analysis of MFA-AMP solid revealed a purity of >90%.

### Synthesis of MFA-CoA Thioester Derivative

The synthesis of MFA-CoA thioesters was accomplished by a method employing ECF.<sup>17, 26</sup> MFA (1.6 mmol) was first dissolved in anhydrous THF (25 ml). While stirring at room temperature, TEA (1.6 mmol) was added to the solution followed by the activation of MFA through the addition of ECF (1.6 mmol). After 30 min, the resulting precipitate, triethylamine hydrochloride, was removed by passing the reaction mixture through a glass funnel fitted with a glass wool plug. The filtered solution was then added to a solution containing CoA (0.13 mmol, 100 mg) and  $\text{KHCO}_3$  (1.6 mmol) in nanopure water (10 ml) and THF (15 ml). The solution was stirred continuously at room temperature for 2 hr, after which the reaction was terminated by acidification (pH 4–5) through the addition of 1N HCl. THF was then removed by evaporation under  $\text{N}_2$  gas. The resulting MFA-CoA underwent solvent washes: acidified water ( $3 \times 10$  ml) and ethyl acetate ( $3 \times 10$  ml). The remaining precipitate was isolated by aspirating the remaining liquid following centrifugation yielding pure MFA-CoA. The MFA-CoA precipitate was blown down to dryness using  $\text{N}_2$  gas and then weighed out for preparation of a 1 mM MFA-CoA solution in DMSO. HPLC analysis of MFA-CoA thioester resulted in an elution time of 7.3 min (Figure 4A) and showed no impurities when analyzed by HPLC/UV (wavelengths: 220, 254, 262, and 280 nm) and LC-MS via reverse-phase gradient elution (as described above). Tandem LC-MS/MS analysis of MFA-CoA standard yielded (CID of  $MH^+$  ion at m/z 991), m/z (%): m/z 582 ( $[M + H - \text{adenosine diphosphate} - \text{H}_2\text{O}]^+$ , 20%), m/z 484 ( $[M + H - \text{adenosine triphosphate}]^+$ , 94%), m/z 382 ( $[M + H - 609]^+$ , 25%), m/z 224 ( $[M + H - \text{CoA}]^+$ , 99%), m/z 428 ( $[\text{adenosine diphosphate} + H]^+$ , 40%), m/z 330 ( $[\text{adenosine monophosphate} + H - \text{H}_2\text{O}]^+$ , 3%).

### Synthesis of MFA-GSH Thioester Derivative

The synthesis of MFA-GSH thioester was performed by the same method as described above for the synthesis of MFA-CoA, with the following exception: CoA was replaced with GSH (1 g) and the resulting precipitate obtained following the evaporation of THF was washed with nanopure water ( $3 \times 50$  ml) to remove any remaining GSH and then by acetone ( $3 \times 50$  ml) to wash away any remaining free MFA and water.<sup>17</sup> The MFA-GSH solid was then blown down to dryness using  $\text{N}_2$  gas and then weighed out for preparation of a 1 mM MFA-GSH solution in DMSO. Product thioester derivatives were characterized by tandem mass spectrometry using the gradient elution as described above. Synthetic MFA-GSH eluted at a retention time of 7.7 min (Figure 4B) and showed no detectable impurities when analyzed by HPLC/UV (wavelengths: 220, 254, 262, and 280 nm) and LC-MS via reverse-phase

gradient elution (as described above). Tandem LC-MS/MS analysis of MFA-GSH standard yielded product in the mass spectrum under collision-induced dissociation (CID) of the protonated molecular ion at  $MH^+$   $m/z$  531,  $m/z$  (%):  $m/z$  456 ( $[M+H - Gly]^+$ , 10%),  $m/z$  384 ( $[M + H - \text{pyroglutamic acid} - \text{water}]^+$ , 82%),  $m/z$  224 ( $[M + H - GSH - \text{water}]^+$ , 73%).

### Incubation Conditions

Chemical stability was assessed by incubating MFA-AMP, MFA-CoA, and MFA-GSH (1  $\mu\text{M}$ ) with CBZ (internal standard) in 0.1 M potassium phosphate buffer (pH 7.4) in 2 ml HPLC vials. The solution was then placed into the HPLC autosampler warmed to 37°C and injections were made every 15 min for 24 h for LC-MS/MS analysis to ascertain the chemical stability of each metabolite. Stability comparisons were made by comparing the analyte peak area to CBZ peak area ratios for each sample. Chemical reactivity experiments ( $n=3$ ) for MFA-AMP, MFA-CoA, and MFA-1-*O*-G were performed by incubating 1  $\mu\text{M}$  of each acyl-linked metabolite separately in 0.1 M potassium phosphate buffer (pH 7.4) containing 10 mM GSH in the absence or presence of equine liver GST (30 units/ml)<sup>27</sup> at 37°C and 0°C (on ice) in screw-capped glass vials in a shaking incubator. Aliquots (100  $\mu\text{l}$ ) of the incubation mixture were taken at 0, 2, 5, 10, 30, and 60 min and quenched with 1  $\mu\text{M}$  CBZ/ACN (100  $\mu\text{M}$ ) solution and then immediately injected onto the column for LC-MS/MS analyses. Quantitative measurements were made using a MFA-GSH standard curve generated from absolute peak areas.

### In Vitro Studies with Rat Hepatocytes

Freshly isolated rat (250–300 g, male Sprague-Dawley) hepatocytes were prepared according to the method of Moldeus et al.<sup>28</sup> and greater than 85% viability was achieved routinely as assessed by trypan blue exclusion testing. Incubations of hepatocytes (2 million viable cells/mL) with MFA (100  $\mu\text{M}$ ) were performed in Williams Media E fortified with L-glutamine (4 mM) in a 50 ml round bottom flask. Incubations ( $n=3$ ) were performed with continuous rotation and gassed with 95%  $\text{O}_2$ /5%  $\text{CO}_2$  at 37°C and 0°C. Aliquots were taken at 0, 0.2, 0.5, 1, 2, 4, 8, 10, 20, 30, and 60 min and analyzed for MFA-AMP, MFA-CoA, MFA-GSH, and MFA-1-*O*-G by LC-MS/MS.

For the analyses of MFA-AMP, MFA-GSH, and MFA-1-*O*-G, aliquots (200  $\mu\text{l}$ ) of the incubation mixture were added directly into microcentrifuge tubes (2 ml) and quenched with a solution of ACN containing 3% formic acid (v/v)/2  $\mu\text{M}$  CBZ (200  $\mu\text{l}$ ). Samples were then centrifuged (14,000 rpm, 5 min) and the supernatant fraction (200  $\mu\text{l}$ ) was transferred to HPLC autosampler vials for LC-MS/MS analysis.

For the analyses of MFA-CoA formation, aliquots (200  $\mu\text{l}$ ) from the same incubations were transferred directly into microcentrifuge tubes and quenched with a solution of acetonitrile containing 2  $\mu\text{M}$  CBZ (400  $\mu\text{l}$ ) followed by the addition of hexane (600  $\mu\text{l}$ ). The samples were vortexed (1 min), centrifuged (14,000 rpm, 5 min), and aliquots (300  $\mu\text{l}$ ) of the aqueous layer were transferred to an HPLC autosampler vial followed by a 1 h evaporation of residual hexane under the fume hood. Samples were then analyzed by LC-MS/MS.

### Identification and Quantification of MFA-AMP

MFA treated rat hepatocyte extracts were analyzed by LC-MS/MS detection for MFA-AMP by multiple reaction monitoring (MRM) transitions  $MH^+$   $m/z$  571 to  $m/z$  224 for MFA-AMP detection (Figure 3B) and  $MH^+$   $m/z$  237 to  $m/z$  194 for CBZ detection using ESI positive ionization mode and the chromatographic methods described above. The elution times of 7.6 min and 9.3 min were obtained for authentic MFA-AMP (Figure 2A) and CBZ, respectively. No chromatographic peaks corresponding to MFA-AMP was detected in blank



incubation extracts lacking MFA. The concentration of MFA-AMP was determined by plotting peak area ratios of MFA-AMP to IS versus the concentration of MFA-AMP.

### Identification and Quantification of MFA-CoA

MFA-treated rat hepatocyte extracts were analyzed by LC-MS/MS for MFA-CoA and CBZ using the multiple reaction monitoring (MRM) transitions  $MH^+$  m/z 991 to m/z 224 for MFA-CoA (Figure 4A) and  $MH^+$  m/z 237 to m/z 194 for CBZ analyses using ESI positive ionization mode and the chromatographic method described above. The elution times of 7.3 min and 9.3 min were obtained for authentic MFA-CoA and CBZ, respectively. No LC-MS/MS chromatographic peak corresponding to MFA-CoA was detected in blank rat hepatocytes incubation extracts. The concentration of MFA-CoA thioester was calculated by plotting peak area ratios of MFA-CoA to IS versus the concentration of MFA-CoA.

### Identification and Quantification of MFA-GSH

MFA-treated rat hepatocyte extracts were analyzed by LC-MS/MS detection for MFA-GSH and CBZ with the use of multiple reaction monitoring (MRM) transitions  $MH^+$  m/z 531 to m/z 224 for MFA-GSH (Figure 4B) and  $MH^+$  m/z 237 to m/z 194 for CBZ detection in ESI positive ionization mode and using the chromatographic methods described above. The elution times of 7.7 min and 9.3 min were obtained for authentic MFA-GSH and CBZ, respectively. No chromatographic peak corresponding to MFA-GSH was detected in blank incubation extracts lacking MFA. The concentration of MFA-GSH was determined by plotting peak area ratios of MFA-GSH to IS versus the concentration of MFA-GSH.

### Identification and Quantification of MFA-1-O-G

MFA-treated rat hepatocytes extracts were analyzed by LC-MS/MS detection for MFA-1-O-G by multiple reaction monitoring (MRM) transitions  $MH^+$  m/z 418 to m/z 224 for MFA-1-O-G and  $MH^+$  m/z 237 to m/z 194 for CBZ detection in ESI positive ionization mode using the chromatographic methods described above. The retention times of 7.9 min and 9.3 min were obtained for authentic MFA-1-O-G (Figure 4C) and CBZ, respectively. No chromatographic peak corresponding to MFA-1-O-G was detected in incubation extracts lacking MFA. The concentration of MFA-1-O-G was determined by plotting peak area ratios of MFA-1-O-G to IS versus the concentration of MFA-1-O-G.

## Results

### Identification of MFA-AMP

Analytical analysis of rat hepatocytes extracts incubated with MFA by LC-MS/MS MRM detection allowed for the identification of MFA-AMP formed in incubations with MFA (Figure 2B). LC-MS/MS analysis revealed the presence of MFA-AMP in MFA incubations with freshly isolated rat hepatocytes. Both MFA-AMP formed in rat hepatocytes extracts and authentic standards coeluted at a retention time of 7.6 min (Figure 2). LC-MS/MS analysis of MFA-AMP formed in rat hepatocytes incubations provided a product ion spectrum where the two major fragment ions were consistent with its chemical structure and were identical to the authentic MFA-AMP standard (Figure 3).

### Identification of MFA-CoA

Analytical analysis of rat hepatocytes extracts by LC-MS/MS MRM detection allowed for the detection of MFA-CoA formation. LC-MS/MS analysis showed the presence of MFA-CoA in rat hepatocytes incubated with MFA, which also coeluted with authentic MFA-CoA standard at a retention time of 7.3 min (Figure 4A). LC-MS/MS analysis of MFA-CoA formation in rat hepatocytes incubations resulted in a product ion spectrum with fragment

ions consistent with its chemical structure and identical to that of authentic MFA-CoA standards (data not shown).

### Identification of MFA-GSH

Analytical analysis of rat hepatocytes extracts incubated with MFA by LC-MS/MS MRM detection made possible the detection of MFA-GSH. LC-MS/MS analysis detected the presence of MFA-GSH in MFA incubations in rat hepatocytes, which eluted at the same time as that of the MFA-GSH authentic standard, retention time of 7.7 min (Figure 4B). LC-MS/MS analysis of MFA-GSH formation in rat hepatocytes incubations resulted in a product ion spectrum with fragment ions consistent with its chemical structure and identical to that of authentic MFA-GSH standards (data not shown).

### Identification of MFA-1-O-G

Analytical analysis of rat hepatocytes extracts of MFA-1-O-G by LC-MS/MS MRM detection allowed for the detection of MFA-1-O-G formed in incubations with MFA. LC-MS/MS analysis revealed the presence of MFA-1-O-G in MFA incubations with freshly isolated rat hepatocytes. Both MFA-1-O-G formed in rat hepatocyte extracts and authentic standards coeluted at a retention time of 7.9 min (Figure 4C). LC-MS/MS analysis of MFA-1-O-G formed in rat hepatocyte incubations provided a product ion spectrum whose fragment ions were consistent with its chemical structure and identical to the authentic MFA-1-O-G standard (data not shown).

### Chemical Stability of MFA-CoA, MFA-AMP, and MFA-GSH in Buffer

In vitro incubation of each acyl-linked metabolite of MFA in potassium phosphate buffer (0.1 M) under physiological conditions (pH 7.4, 37°C) revealed that MFA-AMP, MFA-CoA, and MFA-GSH are chemically stable with no detectable hydrolysis for at least 24 h of incubation (data not shown). Previous studies carried out under the same conditions have shown MFA-1-O-G possesses a half life of degradation of ~16 h in buffer under physiological conditions.<sup>11, 20</sup>

### Reactivity Assessment of MFA-AMP, MFA-CoA, and MFA-1-O-G with GSH in the Presence and Absence of GST in Buffer

Incubation of MFA-AMP with GSH (10 mM) in potassium phosphate buffer (0.1 M) under physiological conditions (pH 7.4, 37°C) resulted in the transacylation of GSH ( $0.21 \pm 0.02$  nM MFA-GSH/min) (Table 1) forming 12.8 nM MFA-GSH at 60 min (Figure 5A). MFA-CoA incubations with GSH revealed an 11-fold greater reactivity for MFA-CoA over the corresponding MFA-AMP ( $2.38 \pm 0.64$  nM MFA-GSH/min), achieving a concentration of 144.9 nM at the 60 min time point (Figure 5B). MFA-1-O-G incubations with GSH resulted in little reactivity with GSH ( $0.02 \pm 0.02$  nM MFA-GSH/min) attaining a concentration of 1.33 nM after 60 min incubation (Figure 5C). Incubations utilizing equine liver GST (30 units/ml) revealed a 6-fold increase in MFA-AMP reactivity (Figure 5A) towards GSH ( $1.25 \pm 0.28$  nM MFA-GSH/min), while incubation of MFA-CoA with GSH in the presence of GST only resulted in a 1.4-fold increase (Figure 5B) in MFA-GSH formation ( $3.38 \pm 0.04$  nM MFA-GSH/min). MFA-1-O-G continued to exhibit little reactivity toward GSH (Figure 5C) in the presence of GST ( $0.07 \pm 0.01$  nM MFA-GSH/min). Reactivity incubations performed in buffer and on ice (0°C, pH 7.4) revealed little to no reactivity for MFA-AMP, MFA-CoA, and MFA-1-O-G in the presence and absence of GST (data not shown).



## Time Course of MFA-AMP, MFA-CoA, MFA-1-O-G, and MFA-GSH Formation in Rat Hepatocytes

The incubation of MFA (100  $\mu\text{M}$ ) in rat hepatocytes under physiological conditions (37°C) resulted in the detection of MFA-AMP in addition to MFA-CoA, MFA-GSH, and MFA-1-O-G (Figure 6A). MFA-GSH formation was quick, reaching a concentration of 1.7  $\mu\text{M}$  at 60 min, while MFA-1-O-G concentrations increased linearly, achieving a concentration of 42.2  $\mu\text{M}$  at 60 min. From the same incubations, MFA-AMP formation was even more rapid and was shown to attain a maximum concentration of 90.2 nM at ~20 sec, whose concentration plateaued thereafter (Figure 6B). MFA-CoA was not detectable until the 4 min time point, reaching a concentration of 45.6 nM at 60 min. Rat hepatocytes experiments incubated on ice (0°C) resulted in an overall decline in the formation for MFA-AMP, MFA-CoA, MFA-1-O-G, and MFA-GSH (Figure 7). The time to maximum concentration for MFA-AMP slowed to 1 min, however MFA-AMP continued to level off at a concentration of 94.1 nM. MFA-CoA levels remained undetectable until 20 min and attained a concentration of 14.1 nM at 60 min. MFA-GSH concentrations experienced a 20-fold decrease (83.9 nM versus 1.7  $\mu\text{M}$  at 60 min), while MFA-1-O-G was nearly undetectable during the course of the incubation.

## Discussion

Mefenamic acid is a fenamic acid derived NSAID prescribed for its analgesic, anti-inflammatory, and antipyretic effects through the inhibition of cyclooxygenase-dependent prostanoid formation.<sup>29</sup> Commonly used for the treatment of pain, MFA has been implicated in several cases of hematologic disturbances including agranulocytosis, hepatic and renal disturbances, nephritis, renal failure, renal papillary necrosis, severe intolerance reactions, and hypersensitivity reactions of the skin and mucous membranes.<sup>30</sup> One potential mechanism for these toxicities is the bioactivation of MFA into reactive acyl-linked metabolites that covalently bind onto macromolecules potentially resulting in an immune-based reaction. MFA is metabolized by cytochrome P450 into the 3-hydroxymethyl-MFA that can either undergo glucuronidation or become further oxidized into the 3-carboxy-MFA, which is primarily excreted unchanged as a monoglucuronide.<sup>9</sup> MFA also undergoes direct conjugative metabolism via the free carboxyl group into the 1-O-acyl glucuronide, MFA-1-O-G, in vitro and in vivo (Figure 1).<sup>9, 10</sup> Studies have shown that MFA-1-O-G irreversibly binds to human serum albumin in vitro and that covalent binding to cellular proteins in culture occurs during the incubation of MFA in the heterologous Chinese hamster lung fibroblast cell line V79 over-expressing UGT1A2.<sup>11</sup> This irreversible binding directly correlates to MFA-1-O-G because nontransfected cells exhibited no covalent binding. In addition to MFA-1-O-G, rat hepatocytes studies have also shown that MFA is metabolized into MFA-CoA and MFA-GSH (Figure 1).<sup>20</sup> Mechanistic studies involving the co-incubation of MFA (10  $\mu\text{M}$ , 10 min) with (-)-borneol (1 mM), an inhibitor of glucuronidation, led to a 91% decrease in MFA-1-O-G formation, however no inhibition of MFA-GSH formation was observed. The co-incubation of MFA with lauric acid (1 mM), an inhibitor of acyl-CoA formation, resulted in a 58% inhibition of MFA-CoA formation but only a 66% inhibition of MFA-GSH formation. These data suggest that an additional intermediate may also play a role in the formation of MFA-GSH. In the present study, we reveal that MFA undergoes bioactivation into the reactive acylating species, MFA-AMP in vitro in rat hepatocytes and we characterized its ability to acylate GSH in comparison to MFA-CoA and MFA-1-O-G.

In order to characterize the conjugative bioactivation products of MFA, it is preferable to use authentic standards. Therefore our initial efforts were dedicated to the synthesis of MFA-AMP, MFA-CoA, and MFA-GSH. MFA-CoA and MFA-GSH were chemically synthesized by conventional procedures commonly utilized in our laboratory employing

ethyl chloroformate,<sup>17, 26</sup> in which the thiol group of CoA and GSH become adducted to MFA via the formation of a mixed anhydride intermediate. The synthetic method for obtaining pure MFA-AMP standards required the selective condensation of the carboxyl function of MFA with the phosphoric acid group of AMP using *N,N'*-dicyclohexylcarbodiimide<sup>31</sup> to form MFA-AMP. Structural confirmation of each MFA standard was authenticated from its LC-MS/MS product ion spectrum.

It is common knowledge that acyl glucuronides are generally less stable than other glucuronides.<sup>32</sup> Hydrolysis and intramolecular acyl migration are two major reactions contributing to this instability that follows first-order kinetics over the measurable concentration range and is predictable based on the degree of substitution at the alpha carbon to the carboxylic acid<sup>12</sup>, and the electron-withdrawing or donating groups at the alpha carbon or on the conjugated aromatic ring. Therefore the previously reported half life of degradation of 16.5 hrs for MFA-1-*O*-G (fully substituted),<sup>11, 20, 30</sup> also confirmed in our laboratory, is consistent with this observation in comparison to the half-life of degradation for the monosubstituted (*S*)-2-phenylpropionic-1- $\beta$ -*O*-acyl glucuronide ( $t_{1/2}$  2.4 hr)<sup>34</sup> and the unsubstituted zomepirac-1- $\beta$ -*O*-acyl glucuronide ( $t_{1/2}$  0.45 hr).<sup>35</sup> The degradation of MFA-1-*O*-G has previously been confirmed to occur primarily through acyl migration and not by hydrolysis.<sup>33</sup> Stability assessment of MFA-CoA revealed it to be highly stable, with no observable hydrolysis, for at least 24 h, which is consistent with previous *S*-acyl-CoA stability data, in which clofibrac acid-*S*-acyl-CoA has been shown to be highly stable in vitro in physiological buffer with a degradation half life of 21 days (~2% hydrolysis/day).<sup>17</sup> Similarly, 2-phenylpropionic-*S*-acyl-CoA<sup>34</sup> and phenylacetyl-*S*-acyl-CoA<sup>36</sup> have also been shown to be completely stable after one day of incubation. MFA-GSH was stable during the 24 h incubation in buffer under physiological conditions, which is expected since *S*-acyl-GSH thioesters are mostly chemically stable products.<sup>17</sup> MFA-AMP was also shown to be chemically stable for the 24 h duration.

The model nucleophile, GSH is a commonly used biomarker of reactivity for bioactivation studies. Glutathione [*N*-(*N*-L- $\gamma$ -glutamyl-L-cysteinyl) glycine] is an endogenous atypical tripeptide that plays a protective role in the body by removing potentially toxic electrophiles.<sup>37</sup> Presumably, the greater the in vitro adduct formation, the greater the probability that the reactive metabolite will covalently bind onto a protein in vivo. The assessment of GSH chemical reactivity reveal that MFA-CoA is 11-fold and 121-fold more reactive towards thiol functional groups than its corresponding MFA-AMP and MFA-1-*O*-G, respectively (Figure 5, Table 1). These data are consistent with previous MFA-CoA and MFA-1-*O*-G reactivity studies<sup>20</sup> and for 2-phenylpropionic acid incubations with GSH resulting in a 70-fold greater GSH reactivity for 2-phenylpropionic-*S*-acyl-CoA compared to its corresponding 2-phenylpropionic-1- $\beta$ -*O*-acyl-glucuronide.<sup>34</sup> Additional studies with cholic acid (CA) have also revealed a higher reactivity of CA-CoA (3.3-fold) with GSH than its complementary CA-AMP.<sup>38</sup> Therefore, the rank order of nonenzymatic in vitro GSH reactivity under physiological conditions was as follows: MFA-CoA > MFA-AMP > MFA-1-*O*-G, demonstrating a more rapid and extensive spontaneous reaction of MFA-CoA thioesters with GSH than its corresponding acyl adenylate and acyl glucuronide derivatives, suggesting that MFA-CoA is predicted to spontaneously contribute more to the covalent binding and possibly an idiosyncratic toxicity than MFA-AMP and MFA-1-*O*-G. Additionally, Mitamura et al. also revealed that the chemical reactivity of acyl-AMP and acyl-CoA intermediates of cholic acid towards model bionucleophiles was selective in that CA-CoAs are more reactive toward the thiol functional groups of GSH and *N*-acetyl-L-cysteine (NAC) while CA-AMP exhibited greater reactivity towards the amino functional groups of glycine and taurine.<sup>38</sup> This preferential reactivity has also been demonstrated in our lab with MFA-AMP, MFA-CoA, MFA-1-*O*-G, and MFA-GSH towards GSH, NAC, glycine, and taurine (manuscript in preparation).

In the presence of the GSH conjugating enzyme, equine liver GST, MFA-AMP reactivity increased 6-fold (Figure 5A, Table 1). Comparatively, GST mediated reactivity of MFA-CoA only increased 1.4-fold (Figure 5B), which is consistent with previously published GST MFA-CoA data (1.3-fold increase).<sup>20</sup> MFA-1-*O*-G continued to show little reactivity in the presence of GST. These data suggest that MFA-AMP is a better substrate for GST than its corresponding MFA-CoA and thus may play a crucial role in the formation of MFA-GSH in the liver. GSH reactivity incubations carried out on ice (0°C) produced little MFA-GSH conjugates, as would be expected.

MFA-AMP is an intermediate in the biosynthesis of MFA-CoA, which is a two-step reaction catalyzed by the actions of acyl-CoA synthetase (ACS) and the cofactors ATP and then CoA. The reaction occurs via a ping-pong mechanism in which the AMP moiety of ATP is transferred to the acyl group forming an acyl-adenylate intermediate and a pyrophosphate (PPi). The enzyme bound activated intermediate is then attacked by CoA to yield the associated acyl-CoA product and free AMP.<sup>39</sup> Previous bioactivation studies of valproic acid in the presence of rat liver mitochondria, ATP, CoA and MgCl<sub>2</sub> resulted in the formation of valproyl-CoA. However, in the absence of CoA, valproyl-AMP was found to exist in its free form.<sup>40</sup> Further studies involving the incubation of R-ibuprofen in rat liver mitochondria also resulted in the formation of the R-ibuprofen-AMP that goes on to form R- and S-ibuprofen-CoA, both of which are substrates for epimerases.<sup>41</sup> However, S-ibuprofen alone was not bioactivated into S-ibuprofen-AMP and its CoA thioester. Further incubations with S-ibuprofen-AMP resulted in the formation of S-ibuprofen-CoA and were also capable of undergoing epimerization into R-ibuprofen-CoA, suggesting that the R-ibuprofen-AMP may be necessary for chiral inversion. In vitro time course of formation in rat hepatocyte studies reveal that MFA indeed undergoes bioactivation to form MFA-AMP as well as MFA-CoA (Figure 6). The incubation of MFA (100 μM) in rat hepatocytes resulted in a rapid formation of MFA-AMP, achieving a maximum concentration of 90.2 nM at ~20 sec, after which the concentration leveled off for the remainder of the 60 min incubation, suggesting saturation of ACS. MFA-CoA was undetectable until the 4 min time point, attaining a concentration of 45.6 nM at 60 min, approximately half the concentration of its intermediate, MFA-AMP. The sequential detection of MFA-AMP (20 sec) followed by MFA-CoA (4 min) is in agreement with the CoA thioester biosynthetic pathway. In addition to MFA-AMP and MFA-CoA, our rat hepatocytes extracts also revealed the linear formation of MFA-1-*O*-G and MFA-GSH achieving a concentration of 42.2 μM and 1.7 μM at the 60 min time point, respectively. In comparison to previous rat hepatocytes time course studies, MFA produces unusually high concentrations of GSH-adducts compared to diclofenac<sup>42</sup>, zomepirac<sup>43</sup>, (R)-ibuprofen<sup>44</sup>, and (R)-flunoxaprofen.<sup>45</sup> MFA-GSH, which is chemically stable in physiological buffer, has previously been shown to possess a metabolic half life of ~8 min in rat hepatocytes.<sup>20</sup> This degradation is likely due to the metabolism of MFA-GSH by endogenous thioesterases or peptidases, due to the lack of detectable *N*-acylcysteinylglycine in these rat hepatocytes extracts, which is consistent with previous studies showing the lack of γ-glutamyl transferase activity in rat livers.<sup>46</sup> The degradation of *S*-acyl-GSH into free acids by GST-mediated hydrolysis is a well documented phenomenon.<sup>47, 48</sup> However, MFA-GSH has been shown to be relatively stable in the presence of equine liver GST (10–11%) after 30 min incubation.<sup>20</sup>

MFA-1-*O*-G and MFA-GSH concentrations both increase linearly over the duration of the 60 min incubation (Figure 6A). However, our previous GSH reactivity studies have shown that MFA-1-*O*-G does not spontaneously nor enzymatically form GSH conjugates (Figure 5C). Therefore, it is unlikely that MFA-1-*O*-G is responsible for the high concentrations of MFA-GSH formed during these incubations, despite its high concentration. Previous incubation studies with zomepirac revealed that zomepirac-1-*O*-acyl glucuronide formation linearly increased over a 2 hr period, achieving an AUC of 2500 μM · min.<sup>43</sup> However,

further studies revealed the time dependent formation of zomepirac-*S*-acyl-GSH is more consistent with the rapid formation of zomepirac-CoA rather than the linear formation of zomepirac-1-*O*-G.<sup>18</sup> Inhibition studies investigating the time course of formation of 2-phenylpropionic-CoA and 2-phenylpropionic-1-*O*-acyl-glucuronide to the overall covalent binding of 2-phenylpropionic acid in rat hepatocytes revealed that complete inhibition of acyl glucuronidation only decreased covalent adduct formation by 18.7% suggesting that the overall covalent binding contribution of acyl glucuronides is small.<sup>49</sup> In our studies, MFA-CoA was not detectable until the 4 min time point and its concentration was 37-fold lower than that of the MFA-GSH (Figure 6A). Therefore, despite its high GSH reactivity, MFA-CoA time course of formation and concentrations are unlikely to account for all of the MFA-GSH formed. Additionally, previous studies utilizing lauric acid as an acyl-AMP and acyl-CoA inhibitor demonstrated that the degree of MFA-CoA inhibition did not completely account for the decrease in its corresponding MFA-GSH<sup>20</sup>, further suggesting that MFA-CoA is not exclusively responsible for the high GSH conjugation associated with MFA. MFA-AMP formation was almost immediate, which is consistent with the fast time course of formation of MFA-GSH, however it being 19-fold lower in concentration than that of MFA-GSH still does not account for the unusually high concentrations of MFA-GSH formed in rat hepatocytes incubations (Figure 6).

Rates of enzyme catalyzed reactions tend to double for every ten degree increase in temperature until the optimal temperature (37°C) is reached. During the incubation of MFA in rat hepatocytes on ice (0°C), UGT activity was completely inhibited, resulting in no MFA-1-*O*-G formation (Figure 7). MFA-CoA was not detectable until 10 min and its concentrations decreased 3.2-fold (14.1 nM). MFA-GSH concentrations decreased 20-fold (83.9 nM), suggesting that GST plays an active role in the formation of GSH adduct in rat hepatocytes. Interestingly, MFA-AMP time to maximum concentration was delayed to 1 min, however its concentrations remained essentially the same during the course of the 60 min incubation. Our reactivity assessments show that MFA-AMP conjugation with GSH is greatly increased in the presence of GST. However, during the course of our rat hepatocyte incubations carried out on ice, MFA-AMP concentrations showed no change while MFA-GSH formation declined greatly, suggesting that GST plays an important role in the formation of MFA-GSH via MFA-AMP. As a result of the rapid speed of MFA-AMP formation (20 sec), we postulate that any MFA-AMP converted into MFA-GSH is quickly replenished and therefore, no changes in the concentration of MFA-AMP are observed during the course of the incubation under physiological conditions. Therefore, we hypothesize that MFA-AMP may be a significant contributor towards the formation of MFA-GSH in rat hepatocytes incubations due to its rapid rate of formation and its high specificity towards GST. However, further studies are still necessary to confirm this phenomenon.

The focus of this study was to characterize and determine the relative contribution that the acyl-adenylate (AMP)-linked intermediates of MFA, MFA-AMP, has on the acylation of the biological nucleophile GSH compared to MFA-CoA and MFA-1-*O*-G in rat liver cells. MFA-AMP was indeed detected in rat hepatocyte incubations, along with its corresponding MFA-CoA and MFA-1-*O*-G. Due to its rapid formation, high affinity toward GST, and consistency in concentration in rat hepatocyte incubations, we propose that MFA-AMP does play a role in the acylation of GSH and may be associated with the covalent binding of MFA to physiological proteins. In addition, previous reactivity studies have shown that acyl-GSH thioesters are reactive intermediates by themselves and are capable of forming covalent bonds to NAC.<sup>17</sup> Since MFA-AMP possesses a high affinity towards GST to form the reactive MFA-GSH thioester, it is feasible that MFA-AMP may play a greater role towards protein adduct formation than our GSH reactivity experiments suggest. Therefore, we speculate that MFA-GSH formation by MFA-AMP via GST may mediate the idiosyncratic

toxicities, either directly or through immune-mediated hypersensitivity reactions, commonly associated with the use of MFA. These results suggest that acyl adenylate formation should be considered in future studies evaluating the potential reactivity of carboxylic acid intermediates.

## Acknowledgments

We would like to thank Dr. Mark Grillo (Amgen Inc., Department of Pharmacokinetics and Drug Metabolism, South San Francisco, CA) for many helpful discussions during the course of this work. We would also like to thank Dr. Vincent Venditto (UCSF, Department of Bioengineering and Therapeutic Sciences) for the NMR characterization of MFA-AMP.

### Funding Source

This work was supported in part by the National Institute of Health Grant GM36633.

## Abbreviations

<b>ACN</b>	acetonitrile
<b>ACS</b>	acyl-CoA synthetase
<b>AMP</b>	adenosine monophosphate
<b>ATP</b>	adenosine triphosphate
<b>CBZ</b>	carbamazepine
<b>CoA</b>	coenzyme A
<b>DMSO</b>	dimethylsulfoxide
<b>ECF</b>	ethyl chloroformate
<b>ESI</b>	electrospray ionization
<b>GSH</b>	L-glutathione
<b>GST</b>	glutathione-S-transferase
<b>HPLC</b>	high performance liquid chromatography
<b>LC-MS/MS</b>	liquid chromatography mass spectrometry
<b>MFA</b>	mefenamic acid
<b>MFA-AMP</b>	mefenamic acid-acyl-adenylate
<b>MFA-S-acyl-CoA</b>	mefenamic acid-S-acyl-Coenzyme A
<b>MFA-GSH</b>	mefenamic acid-S-acyl-glutathione
<b>MFA-1-O-G</b>	mefenamic acid-1-O-acyl-glucuronide
<b>MRM</b>	multiple reaction monitoring
<b>NAC</b>	N-acetyl-L-cysteine
<b>NSAID</b>	nonsteroidal anti-inflammatory drug
<b>TEA</b>	triethylamine
<b>THF</b>	tetrahydrofuran



## References

1. Bakke OM, Wardell WM, Lasagna L. Drug discontinuations in the United Kingdom and the United States, 1964 to 1983: issues of safety. *Clin Pharmacol Ther.* 1984; 35:559–567. [PubMed: 6713769]
2. Zimmerman HJ. Update of hepatotoxicity due to classes of drugs in common clinical use: non-steroidal drugs, anti-inflammatory drugs, antibiotics, antihypertensives, and cardiac and psychotropic agents. *Semin Liver Dis.* 1990; 10:322–338. [PubMed: 2281340]
3. Zimmerman, HJ. Hepatic Injury Associated with Nonsteroidal Anti-Inflammatory Drugs. In: Lewis, AJ.; Furst, DE., editors. *Nonsteroidal Antiinflammatory Drugs: Mechanism and Clinical Use.* Marcel Dekker Inc; New York: 1994. p. 171-194.
4. Bakke OM, Manocchia M, De Abajo F, Kaitin KI, Lasagna L. Drug safety discontinuations in the United Kingdom, the United States, and Spain from 1974 through 1993: a regulatory perspective. *Clin Pharmacol Ther.* 1995; 58:108–117. [PubMed: 7628177]
5. Zimmerman, HJ. *Hepatotoxicity: The Adverse Effects of Drugs and Other Chemicals on the Liver.* Lippincott Williams & Wilkins; Philadelphia: 1999.
6. Calvey N. Adverse drug reactions. *Anaesth Int Care Med.* 2005; 6:245–249.
7. Pirmohamed M. Genetic factors in the predisposition to drug-induced hypersensitivity reactions. *AAPS J.* 2006; 8:E20–E26. [PubMed: 16584129]
8. Somchit N, Sanat F, Gan EH, Shahrin IA, Zuraini A. Liver injury induced by the non-steroidal anti-inflammatory drug mefenamic acid. *Singapore Med J.* 2004; 45:530–532. [PubMed: 15510325]
9. Glazko AJ. Experimental observations on flufenamic, mefenamic and meclofenamic acids. 3. Metabolic disposition. *Ann Phys Med Suppl.* 1966:23–36.
10. Sato J, Yamane Y, Ito K, Bando H. Structures of mefenamic acid metabolites from human urine. *Biol Pharm Bull.* 1993; 16:811–812. [PubMed: 8220331]
11. McGurk KA, Rimmel RP, Hogagrahara VP, Tosh D, Burchell B. Reactivity of mefenamic acid 1-*O*-acyl glucuronide with proteins in vitro and ex vivo. *Drug Metab Dispos.* 1996; 24:842–849. [PubMed: 8869817]
12. Benet LZ, Spahn-Langguth H, Iwakawa S, Volland C, Mizuma T, Mayer S, Mutschler E, Lin ET. Predictability of the covalent binding of acidic drugs in man. *Life Sci.* 1993; 53:PL141–146. [PubMed: 8350674]
13. Shore LJ, Fenselau C, King AR, Dickinson RG. Characterization and formation of the glutathione conjugate of clofibric acid. *Drug Metab Dispos.* 1995; 23:119–123. [PubMed: 7720514]
14. Tang W, Borel AG, Abbott FS. Conjugation of glutathione with a toxic metabolite of valproic acid, (E)-2-propyl-2,4-pentadienoic acid, catalyzed by rat hepatic glutathione-*S*-transferases. *Drug Metab Dispos.* 1996; 24:436–446. [PubMed: 8801059]
15. Wang W, Ballatori N. Endogenous glutathione conjugates: occurrence and biological functions. *Pharmacol Rev.* 1998; 50:335–356. [PubMed: 9755286]
16. Olsen J, Bjornsdottir I, Tjornelund J, Honore Hansen S. Chemical reactivity of the naproxen acyl glucuronide and the naproxen coenzyme A thioester towards bionucleophiles. *J Pharm Biomed Anal.* 2002; 29:7–15. [PubMed: 12062660]
17. Grillo MP, Benet LZ. Studies on the reactivity of clofibryl-*S*-acyl-CoA thioester with glutathione in vitro. *Drug Metab Dispos.* 2002; 30:55–62. [PubMed: 11744612]
18. Grillo MP, Hua F. Identification of zomepirac-*S*-acyl-glutathione in vitro in incubations with rat hepatocytes and in vivo in rat bile. *Drug Metab Dispos.* 2003; 31:1429–1436. [PubMed: 14570776]
19. Sidenius U, Skonberg C, Olsen J, Hansen SH. In vitro reactivity of carboxylic acid-CoA thioesters with glutathione. *Chem Res Toxicol.* 2004; 17:75–81. [PubMed: 14727921]
20. Grillo MP, Tadano Lohr M, Wait JC. Metabolic activation of mefenamic acid leading to mefenamyl-*S*-acyl-glutathione adduct formation in vitro and in vivo in rat. *Drug Metab Dispos.* 2012; 40:1515–1526. [PubMed: 22577085]
21. Kelley M, Vessey DA. Characterization of the acyl-CoA:amino acid *N*-acyltransferases from primate liver mitochondria. *J Biochem Toxicol.* 1994; 9:153–158. [PubMed: 7983681]



22. Mano N, Uchida M, Okuyama H, Sasaki I, Ikegawa S, Goto J. Simultaneous detection of cholyl adenylate and coenzyme A thioester utilizing liquid chromatography/electrospray ionization mass spectrometry. *Anal Sci.* 2001; 17:1037–1042. [PubMed: 11708055]
23. Ikegawa S, Ishikawa H, Oiwa H, Nagata M, Goto J, Kozaki T, Gotowda M, Asakawa N. Characterization of cholyl-adenylate in rat liver microsomes by liquid chromatography/electrospray ionization-mass spectrometry. *Anal Biochem.* 1999; 266:125–132. [PubMed: 9887221]
24. Goto J, Nagata M, Mano N, Kobayashi N, Ikegawa S, Kiyonami R. Bile acid acyl adenylate: a possible intermediate to produce a protein-bound bile acid. *Rapid Commun Mass Spectrom.* 2001; 15:104–109. [PubMed: 11180537]
25. Takamura-Enya T, Mano N, Kawahara N, Goto J, Wakabayashi K. Formation of DNA adducts with cholyl adenylate, a putative intermediate for biosynthesis of cholyl-CoA. *Chem Res Toxicol.* 2005; 18:1715–1720. [PubMed: 16300380]
26. Stadtman TC, Elliott P. Studies on the enzymic reduction of amino acids. II Purification and properties of D-proline reductase and a proline racemase from *Clostridium sticklandii*. *J Biol Chem.* 1957; 228:983–997. [PubMed: 13475375]
27. Kalgutkar AS, Mascitti V, Sharma R, Walker GW, Ryder T, McDonald TS, Chen Y, Preville C, Basak A, McClure KF, Kohrt JT, Robinson RP, Munchhof MJ, Cornelius P. Intrinsic electrophilicity of a 4-substituted-5-cyano-6-(2-methylpyridin-3-yloxy)pyrimidine derivative: structural characterization of glutathione conjugates in vitro. *Chem Res Toxicol.* 2011; 24:269–278. [PubMed: 21288051]
28. Moldeus P, Jones DP, Ormstad K, Orrenius S. Formation and metabolism of a glutathione-S-conjugate in isolated rat liver and kidney cells. *Biochem Biophys Res Commun.* 1978; 83:195–200. [PubMed: 697808]
29. Hawkey CJ, Yeomans ND. The treatment and prophylaxis of nonsteroidal anti-inflammatory drug (NSAID)-associated ulcers and erosions. *Can J Gastroenterol.* 1999; 13:291–295. [PubMed: 10400490]
30. Handisurya A, Moritz KB, Riedl E, Reinisch C, Stingl G, Wohrl S. Fixed drug eruption caused by mefenamic acid: a case series and diagnostic algorithms. *J Dtsch Dermatol Ges.* 2011; 9:374–378. [PubMed: 21366861]
31. Berg P. The chemical synthesis of amino acyl adenylates. *J Biol Chem.* 1958; 233:608–611. [PubMed: 13575422]
32. Spahn-Langguth H, Benet LZ. Acyl glucuronides revisited: is the glucuronidation process a toxification as well as a detoxification mechanism? *Drug Metab Rev.* 1992; 24:5–47. [PubMed: 1555494]
33. Walker GS, Atherton J, Bauman J, Kohl C, Lam W, Reily M, Lou Z, Mutlib A. Determination of degradation pathways and kinetics of acyl glucuronides by NMR spectroscopy. *Chem Res Toxicol.* 2007; 20:876–886. [PubMed: 17536843]
34. Li C, Benet LZ, Grillo MP. Studies on the chemical reactivity of 2-phenylpropionic acid 1-O-acyl glucuronide and S-acyl-CoA thioester metabolites. *Chem Res Toxicol.* 2002; 15:1309–1317. [PubMed: 12387630]
35. Fenselau, C. Acyl Glucuronides as Chemically Reactive Intermediates. In: Kauffman, FC., editor. *Conjugation-Deconjugation Reactions in Drug Metabolism and Toxicity.* Springer-Verlag; Berlin: 1994. p. 367-389.
36. Grillo MP, Lohr MT. Covalent binding of phenylacetic acid to protein in incubations with freshly isolated rat hepatocytes. *Drug Metab Dispos.* 2009; 37:1073–1082. [PubMed: 19196839]
37. Ionescu, C.; Caira, M. *Drug Metabolism, Current Concepts.* Springer; Dordrecht: 2005.
38. Mitamura K, Aoyama E, Sakai T, Iida T, Hofmann AF, Ikegawa S. Characterization of non-enzymatic acylation of amino or thiol groups of bionucleophiles by the acyl-adenylate or acyl-CoA thioester of cholic acid. *Anal Bioanal Chem.* 2011; 400:2253–2259. [PubMed: 21491109]
39. Vlahcevic ZR, Pandak WM, Stravitz RT. Regulation of bile acid biosynthesis. *Gastroenterol Clin North Am.* 1999; 28:1–25. [PubMed: 10198776]

40. Mao LF, Millington DS, Schulz H. Formation of a free acyl adenylate during the activation of 2-propylpentanoic acid. valproyl-AMP: a novel cellular metabolite of valproic acid. *J Biol Chem.* 1992; 267:3143–3146. [PubMed: 1737769]
41. Menzel S, Waibel R, Brune K, Geisslinger G. Is the formation of R-ibuprofenyl-adenylate the first stereoselective step of chiral inversion? *Biochem Pharmacol.* 1994; 48:1056–1058. [PubMed: 8093095]
42. Grillo MP, Hua F, Knutson CG, Ware JA, Li C. Mechanistic studies on the bioactivation of diclofenac: identification of diclofenac-S-acyl-glutathione in vitro in incubations with rat and human hepatocytes. *Chem Res Toxicol.* 2003; 16:1410–1417. [PubMed: 14615966]
43. Olsen J, Li C, Bjornsdottir I, Sidenius U, Hansen SH, Benet LZ. In vitro and in vivo studies on acyl-coenzyme A-dependent bioactivation of zomepirac in rats. *Chem Res Toxicol.* 2005; 18:1729–1736. [PubMed: 16300382]
44. Grillo MP, Hua F. Enantioselective formation of ibuprofen-S-acyl-glutathione in vitro in incubations of ibuprofen with rat hepatocytes. *Chem Res Toxicol.* 2008; 21:1749–1759. [PubMed: 18680316]
45. Grillo MP, Wait JC, Tadano Lohr M, Khera S, Benet LZ. Stereoselective flunoxaprofen-S-acyl-glutathione thioester formation mediated by acyl-CoA formation in rat hepatocytes. *Drug Metab Dispos.* 2010; 38:133–142. [PubMed: 19786506]
46. Hinchman CA, Ballatori N. Glutathione-degrading capacities of liver and kidney in different species. *Biochem Pharmacol.* 1990; 40:1131–1135. [PubMed: 1975172]
47. Dietze EC, Grillo MP, Kalthorn T, Nieslanik BS, Jochheim CM, Atkins WM. Thiol ester hydrolysis catalyzed by glutathione S-transferase A1-1. *Biochemistry.* 1998; 37:14948–14957. [PubMed: 9778372]
48. Ibarra C, Grillo MP, LoBello M, Nucetelli M, Bammler TK, Atkins WM. Exploration of in vitro pro-drug activation and futile cycling by glutathione S-transferases: thiol ester hydrolysis and inhibitor maturation. *Arch Biochem Biophys.* 2003; 414:303–311. [PubMed: 12781783]
49. Li C, Benet LZ, Grillo MP. Enantioselective covalent binding of 2-phenylpropionic acid to protein in vitro in rat hepatocytes. *Chem Res Toxicol.* 2002; 15:1480–1487. [PubMed: 12437340]

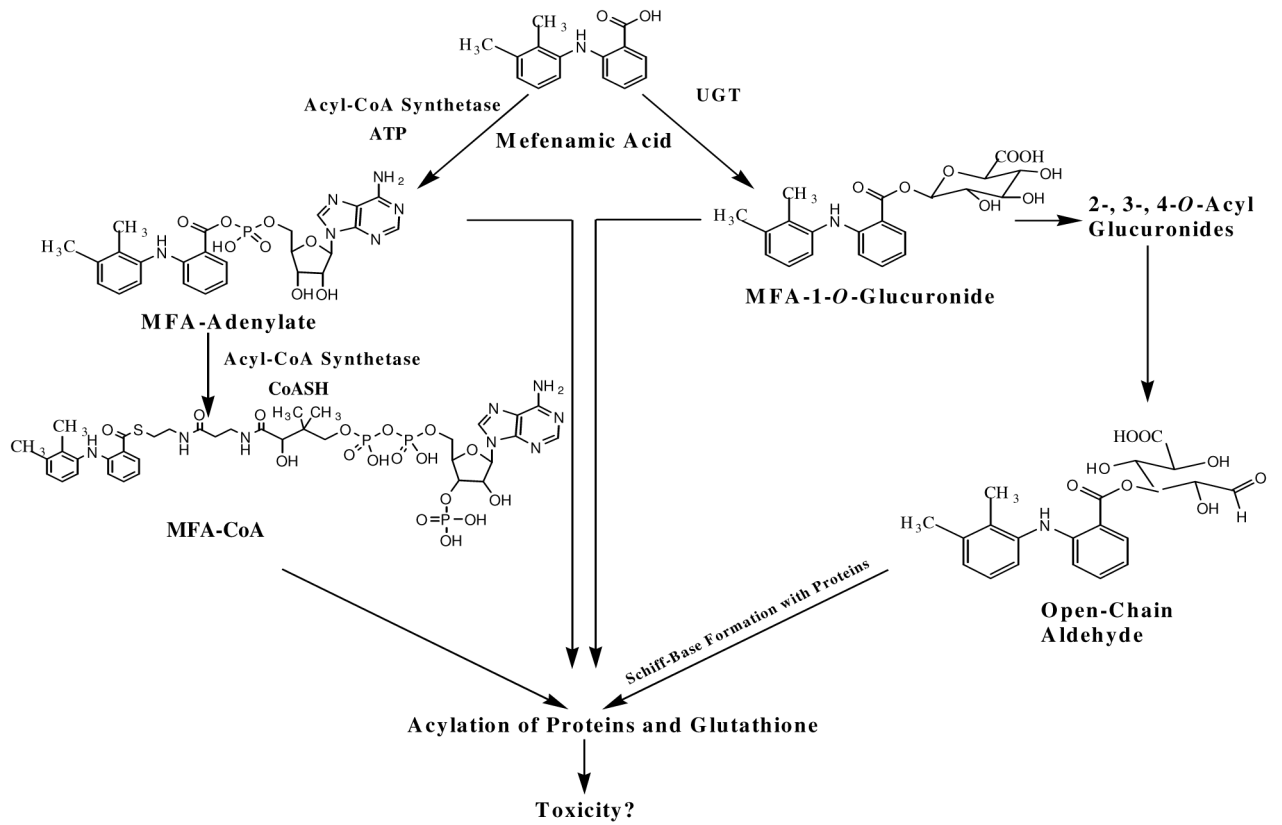


**Figure 1.**  
Proposed conjugative bioactivation routes of mefenamic acid

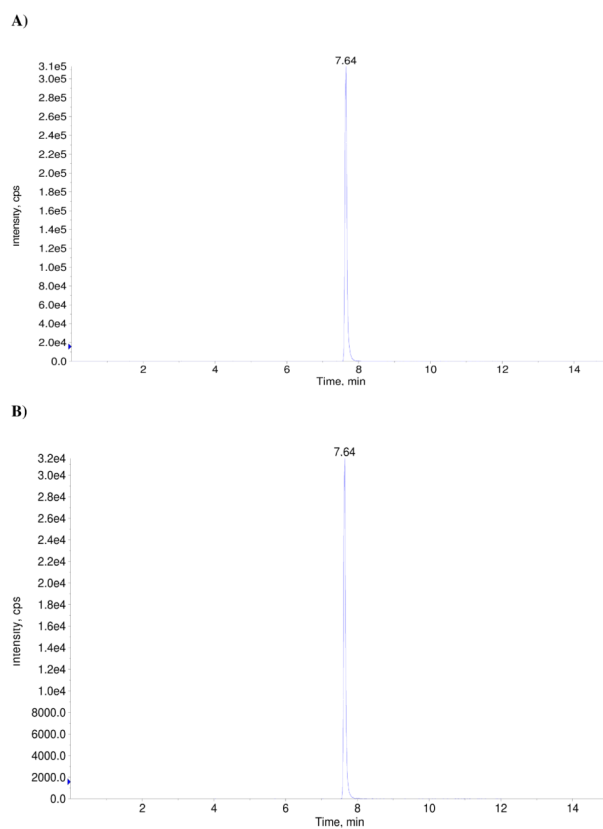


**Figure 2.** Representative reverse-phase gradient LC-MS/MS Single Reaction Monitoring (SRM) ( $m/z$  571 to  $m/z$  224) of MFA-AMP (A) authentic standard and MFA-AMP (B) biologically formed in rat hepatocytes.

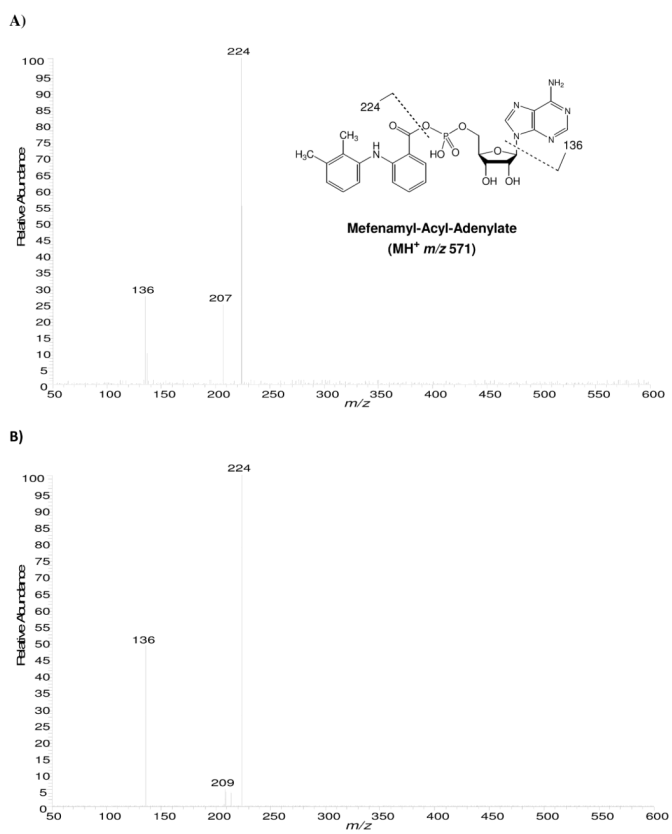
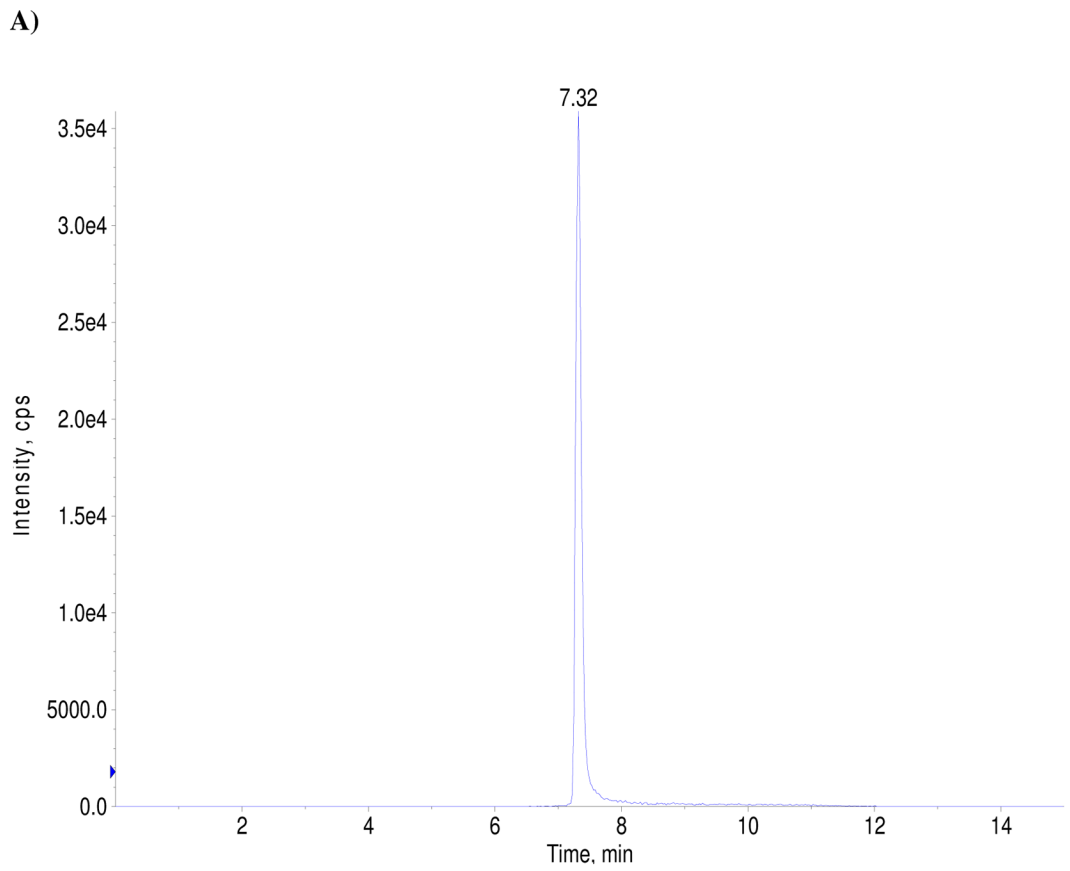
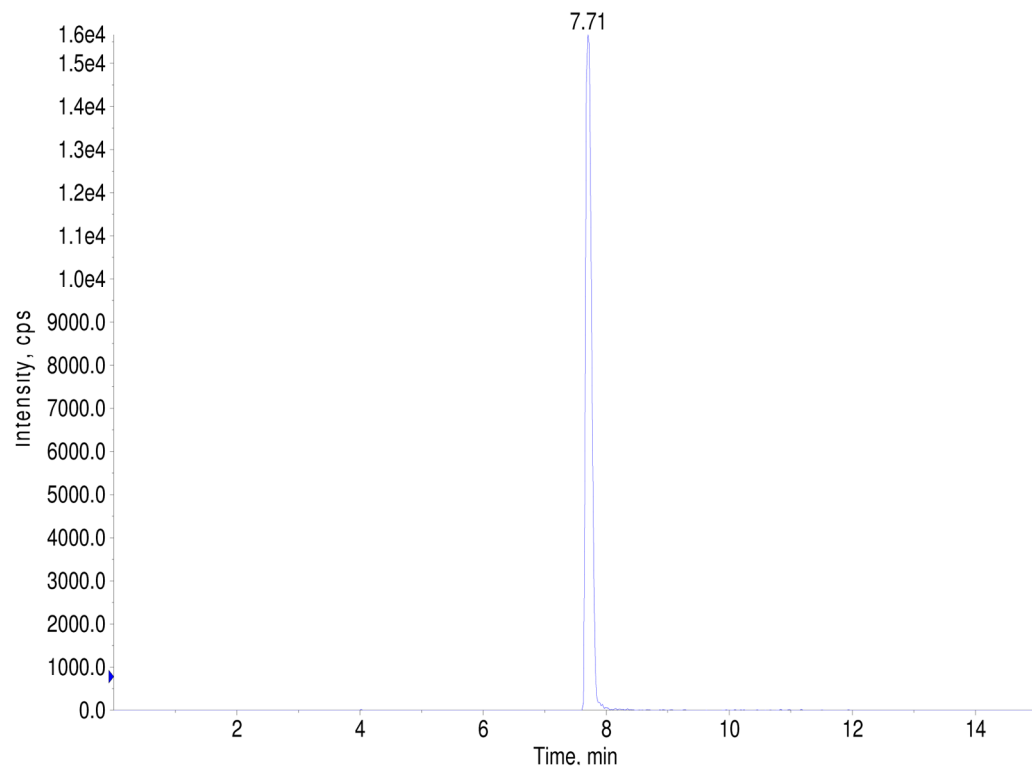


**Figure 3.** Tandem mass spectrum of MFA-AMP (A) authentic standard and MFA-AMP (B) biologically formed in rat hepatocytes.





**B)**



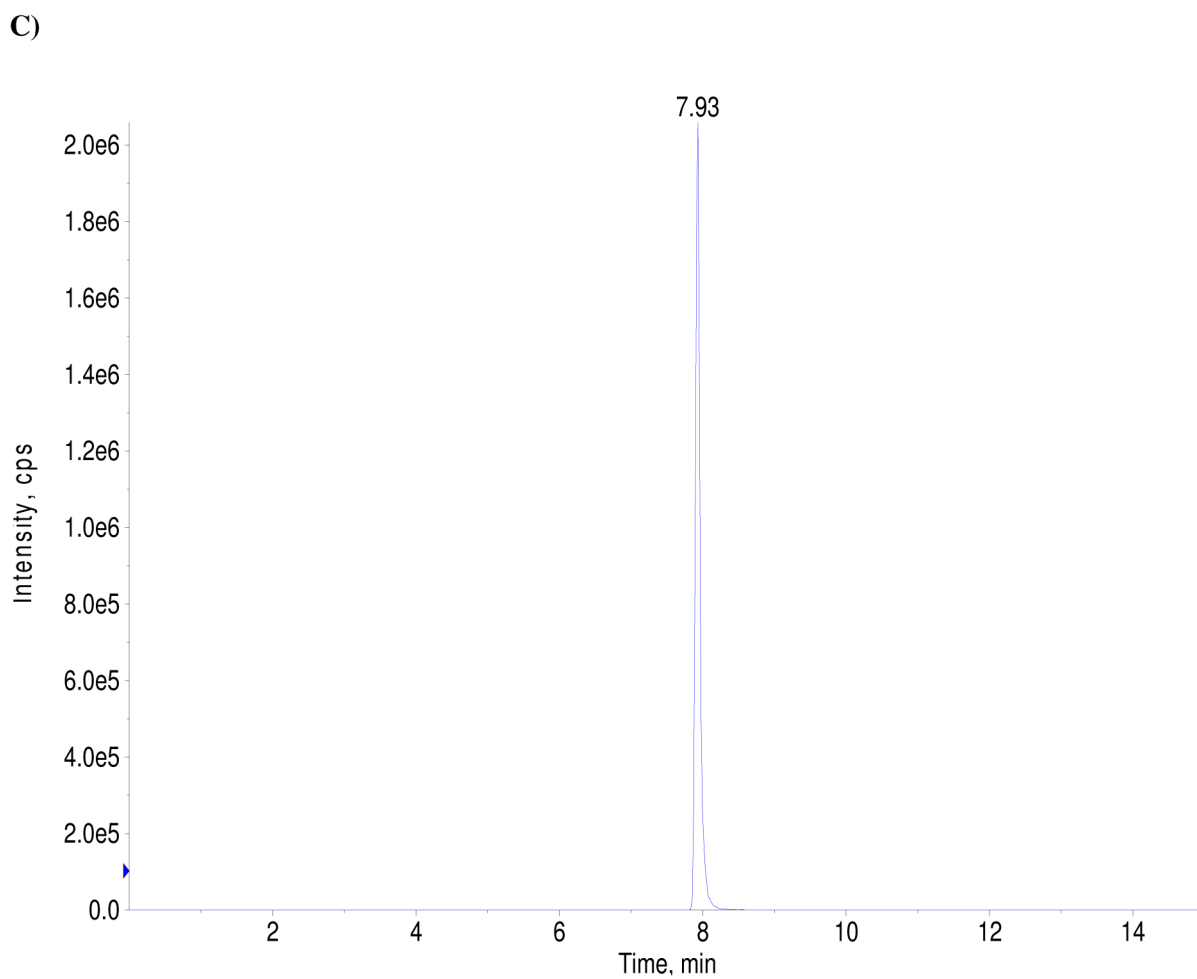


**Figure 4.** Representative reverse-phase gradient LC-MS/MS Single Reaction Monitoring (SRM) of (A) MFA-CoA (m/z 991 to m/z 224), (B) MFA-GSH (m/z 531 to m/z 224), and (C) MFA-1-O-G (m/z 418 to m/z 242) authentic standards.

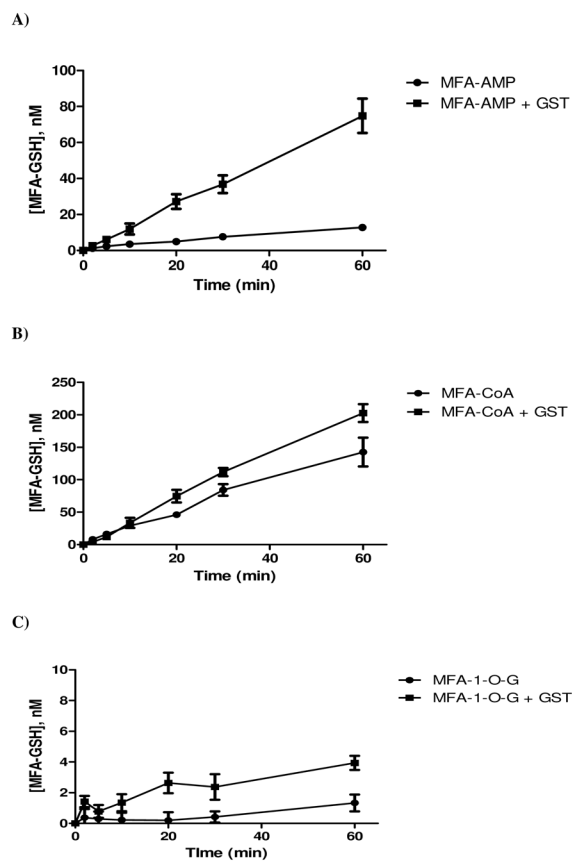


**Figure 5.** Mean reactivity assessment  $\pm$  standard deviations of A) MFA-AMP, B) MFA-CoA, and C) MFA-1-O-G (1  $\mu$ M) with or without equine liver GST (30 U/ml) in 10 mM GSH/0.1 M Kpi (pH 7.4, 37°C).

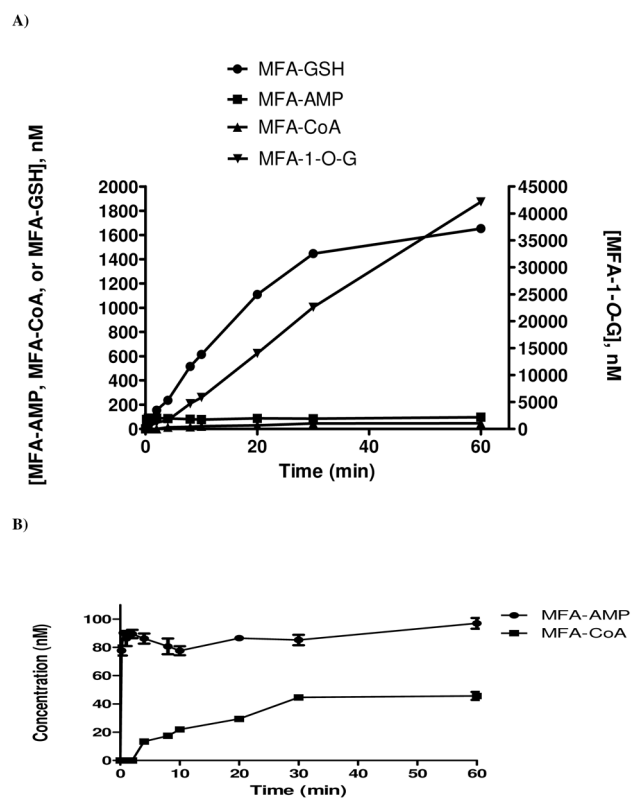


**Figure 6.** Mean time-dependent formation  $\pm$  standard deviations of (A) MFA-AMP, MFA-CoA, MFA-1-*O*-G, and MFA-GSH and (B) MFA-AMP and MFA-CoA in rat hepatocytes incubation (pH 7.4, 37°C) (MFA dose 100  $\mu$ M).

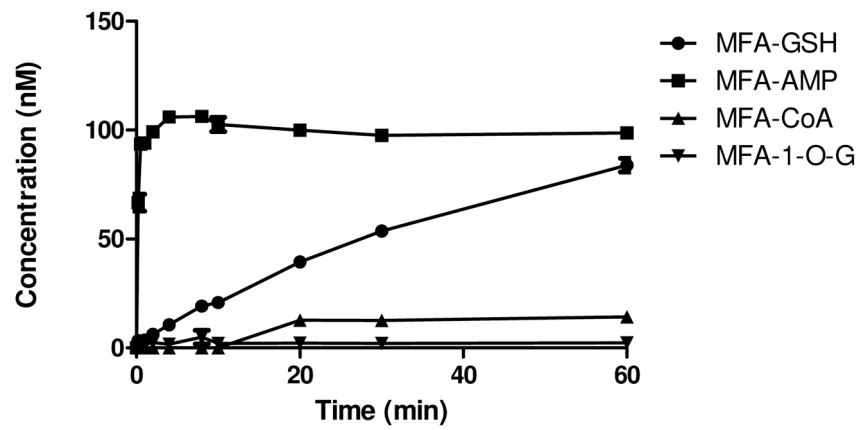


**Figure 7.** Mean time-dependent formation  $\pm$  standard deviations of MFA-conjugates in rat hepatocyte incubations on ice (pH 7.4, 0°C).

**Table 1**

Mean rates  $\pm$  standard deviations of formation of MFA-GSH in physiological buffer (pH 7.4, 37°C) (n=3).

Derivative (1 $\mu$ M)	MFA-GSH Formation (nM/min)
MFA-AMP	0.21 $\pm$ 0.02
MFA-AMP + GST	1.25 $\pm$ 0.28
MFA-CoA	2.41 $\pm$ 0.64
MFA-CoA + GST	3.38 $\pm$ 0.04
MFA-1-O-Gluc	0.02 $\pm$ 0.02
MFA-1-O-Gluc + GST	0.07 $\pm$ 0.01